Cancer Cell
Article

Somatic Single Hits Inactivate the X-Linked Tumor Suppressor *FOXP3* in the Prostate

Lizhong Wang,[1,5] Runhua Liu,[1,5] Weiquan Li,[1] Chong Chen,[1] Hiroto Katoh,[1] Guo-Yun Chen,[1] Beth McNally,[1] Lin Lin,[1] Penghui Zhou,[1] Tao Zuo,[4] Kathleen A. Cooney,[2] Yang Liu,[1,2,*] and Pan Zheng[1,3,*]
[1]Division of Immunotherapy, Department of Surgery
[2]Department of Internal Medicine
[3]Department of Pathology
University of Michigan School of Medicine and Cancer Center, Ann Arbor, MI 48109, USA
[4]Department of Molecular Virology, Immunology, and Medical Genetics, The Ohio State University Medical Center, Columbus, OH 43210, USA
[5]These authors contributed equally to this work
*Correspondence: yangl@umich.edu (Y.L.), panz@umich.edu (P.Z.)
DOI 10.1016/j.ccr.2009.08.016

SUMMARY

Despite clear epidemiological and genetic evidence for X-linked prostate cancer risk, all prostate cancer genes identified are autosomal. Here, we report somatic inactivating mutations and deletion of the X-linked *FOXP3* gene residing at Xp11.23 in human prostate cancer. Lineage-specific ablation of *FoxP3* in the mouse prostate epithelial cells leads to prostate hyperplasia and prostate intraepithelial neoplasia. In both normal and malignant prostate tissues, FOXP3 is both necessary and sufficient to transcriptionally repress c*MYC*, the most commonly overexpressed oncogene in prostate cancer as well as among the aggregates of other cancers. *FOXP3* is an X-linked prostate tumor suppressor in the male. Because the male has only one X chromosome, our data represent a paradigm of "single genetic hit" inactivation-mediated carcinogenesis.

INTRODUCTION

Genetic lesions of several autosomal tumor suppressor genes, including *PTEN* (Sansal and Sellers, 2004; Suzuki et al., 1998), *NKX3.1* (Emmert-Buck et al., 1995; Vocke et al., 1996), and *KLF6* (Bar-Shira et al., 2006; Narla et al., 2005; Narla et al., 2001), have been implicated in the molecular pathogenesis of prostate cancer. In addition, epidemiological studies have suggested a role for X-linked genes that control the susceptibility to prostate cancer (Monroe et al., 1995). Although two loci, one in Xp11.22 (Gudmundsson et al., 2008) and one in Xq27-28 (Xu et al., 1998), have been implicated, the genes in these regions have not been identified. X-linked tumor suppressor genes are of particular interest because the majority of X-linked genes are dose compensated, making a single hit sufficient to inactivate their functions (Spatz et al., 2004). Although we and others have reported X-linked tumor suppressor genes, *WTX1* (Rivera et al., 2007) and *FOXP3* (residing at Xp11.23) (Zuo et al., 2007b) in female cancer patients, none have been identified for cancer in male patients.

In addition to inactivation of tumor suppressors, activation of proto-oncogenes also play a critical role in carcinogenesis. Among them, *c-MYC* (hereby called *MYC*) is known as one of the most commonly overexpressed oncogenes. *MYC* overexpression occurs in more than 30% of all human cancer cases studied (Grandori et al., 2000). However, the mechanism by which *MYC* transcription is increased in the prostate cancer remains unclear. In Burkitt's lymphoma, the *MYC* locus is translocated into a constitutively active Ig locus (Dalla-Favera et al., 1982; Taub et al., 1982), which was found to lead to its transcriptional activation (Erikson et al., 1983). In lung cancer, high levels of gene amplification of the *MYC* locus have been documented (Wong et al., 1986), although such amplification occurred considerably less frequently than overexpression of *MYC* mRNA (Takahashi et al., 1989). Likewise, in breast and prostate cancer, upregulation of *MYC* mRNA was substantially more frequent than amplification of the *MYC* gene (Bieche et al., 1999; Jenkins et al., 1997; Latil et al., 2000). Because *MYC* has been shown to be a target of β-catenin activation (He et al., 1998; Sansom et al., 2007), an appealing hypothesis is that MYC upregulation may be a manifestation of aberrant Wnt

SIGNIFICANCE

The study describes two significant advances. First, we demonstrate *FOXP3* as an X-linked tumor suppressor gene in the male in both human and mice. Because the male has only one X chromosome, our work represents a compelling exception to the widely accepted "two hit" theory for inactivation of tumor suppressor genes. Second, our work demonstrates that FOXP3 is a major transcriptional repressor of *c-MYC* oncogene in the prostate. *FOXP3* inactivation is necessary and sufficient for *c-MYC* overexpression, which is critical for molecular pathogenesis of prostate cancer.

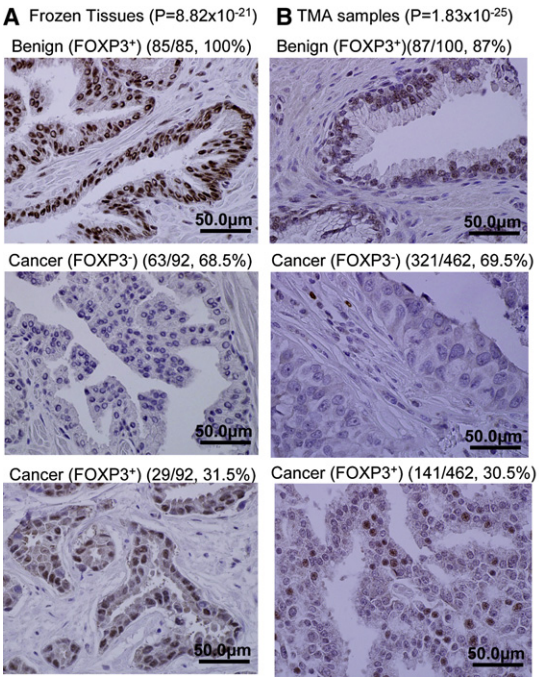

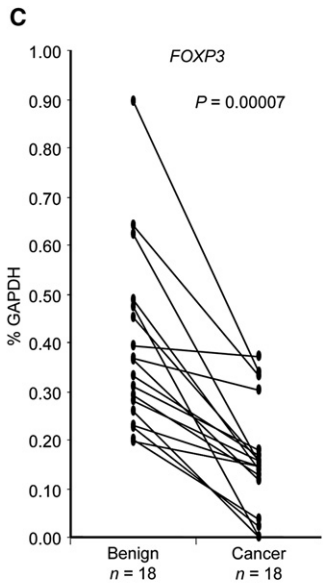

Figure 1. Downregulation of FOXP3 in Prostate Cancer

(A and B) Loss of FOXP3 expression in prostate cancer samples. Data show IHC data for FOXP3 expression in benign versus cancerous tissue in either thawed frozen tissues after short-term formalin fixation (A) or TMA samples after an extended antigen retrieval (B), using monoclonal anti-FOXP3 mAb (236A/E7, 1:100). Statistical significance was analyzed by chi-square tests.

(C) Downregulation of *FOXP3* transcripts in primary cancer tissue in comparison to normal prostate tissue from the same patients (p value by a Wilcoxon two-sample test). Data show real-time PCR quantitation of microdissection samples from 18 cases. The relative amounts are expressed as a percentage of *GAPDH*.

signaling, which occurs frequently in a variety of cancers (Fearon and Dang, 1999). However, a general significance of β-catenin-mediated *MYC* upregulation remains to be demonstrated (Kolligs et al., 1999; Bommer and Fearon, 2007). Therefore, for the majority of cancer types, the genetic change involved in the aberrant *MYC* expression remained to be defined.

MYC overexpression in benign prostate hyperplasia and prostate cancer was documented over 20 years ago (Fleming et al., 1986). Ectopic expression of MYC causes hyperplasia of prostate tissue (Thompson et al., 1989). Further studies demonstrated that *Myc* and *Ras* in combination could induce prostate cancer in mice (Lu et al., 1992). More recently, gene expression profiling of a mouse prostate cancer model induced by *Myc* transgene indicated similarity with human prostate cancer (Ellwood-Yen et al., 2003). Consistent with a role for *MYC* in the pathogenesis of prostate cancer, several whole genome scanning studies have strongly implicated a region 260 kb telomeric to the *MYC* gene in susceptibility to prostate cancer (Amundadottir et al., 2006; Gudmundsson et al., 2007; Haiman et al., 2007a; Haiman et al., 2007b; Witte, 2007; Yeager et al., 2007).

Here, we investigated whether the *FOXP3* gene is frequently inactivated in prostate cancer samples by deletion and somatic mutation. Moreover, we determined the significance of such inactivation by growth inhibition of normal and cancerous prostate cell lines and by identification of FOXP3 targets. The impact of prostate-specific ablation of the *FoxP3* gene in the mouse was also tested.

RESULTS

Somatic Inactivation of the *FOXP3* Locus in Human Prostate Cancer Samples

We first evaluated the expression of FOXP3 in both normal and malignant prostate tissues by immunohistochemistry. Although our previous studies have demonstrated the expression of FoxP3 in the mouse prostate using an affinity-purified anti-FoxP3 peptide antibody (Chen et al., 2008), the FOXP3 expression was not reported in either normal or malignant human prostate tissues by immunohistochemistry (IHC), even though FOXP3 expression on infiltrating regulatory T cells was clearly detectable (Fox et al., 2007; Roncador et al., 2005). As the master regulator of regulatory T cells, *FoxP3* is expressed there at levels comparable to those of housekeeping genes, such as *GAPDH* and *HPRT* (Fontenot et al., 2003; Hori et al., 2003). Because *FoxP3* expression in prostate tissue is approximately 100-fold lower than what was found in regulatory T cells (Chen et al., 2008), we reasoned that the lack of detectable FOXP3 in normal prostate tissue may be caused by low sensitivity of staining and/or tissue processing conditions. Therefore, we first fixed the frozen tissues in 10% formalin for 8–12 hr and screened a large panel of commercially available anti-FOXP3 antibodies for their reactivity to endogenous FOXP3 in epithelial tissues. A shown in Figure S1 (available with this article online), anti-FOXP3 mAb stained prostate epithelial uniformly. However, compared with infiltrating lymphocytes, the level of FOXP3 is considerably lower (Figure S2).

As summarized in Table S1, four commercially available mAbs gave uniform staining of FOXP3 in normal prostate epithelia. The fact that multiple anti-FOXP3 mAbs reacted to FOXP3 demonstrated that FOXP3 is expressed at significant levels in normal prostate tissue. Among them, two (hFOXY and 236A/E7) were also tested and found to react specifically with FOXP3 protein in western blot of lysates made from immortalized mammary epithelial cell line MCF-10A. The specificity of the reactivity to human FOXP3 was further confirmed by comparing reactivity of scrambled and *FOXP3* ShRNA-transduced normal epithelial cell line MCF10A by western blot and by IHC (Figure S3).

Using the uniform fixation and processing conditions, we evaluated the expression of FOXP3 in 85 cases of normal and 92 cases of cancer tissues. As shown in Figure 1A, immunohistochemistry with anti-FOXP3 mAb detected nuclear FOXP3 staining in 100% of the normal prostate tissues tested. In contrast, only 31.5% of the prostate cancer samples show nuclear

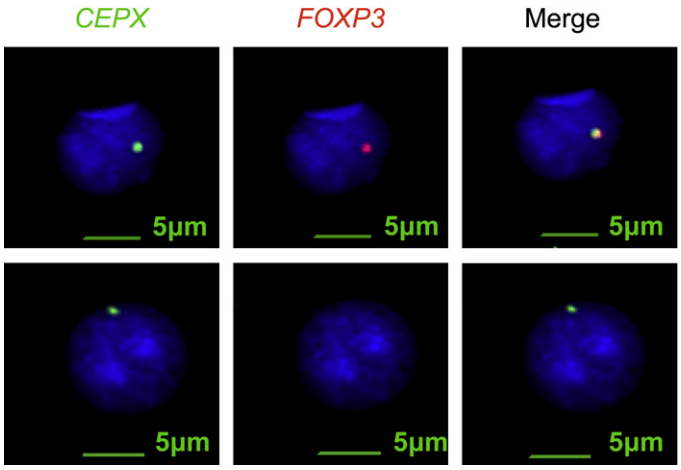

Figure 2. Deletion of a *FOXP3* Among Prostate Cancer Samples

TMA and frozen samples were hybridized to the *FOXP3* (red) or X chromosome probe (green). Of 165 cases with informative FISH data, a total of 23 cases showed *FOXP3* deletion.

FOXP3 staining ($p = 8.82 \times 10^{-21}$). Perhaps as a result of harsher fixation conditions in preparing samples for tissue microarrays, the FOXP3 protein was generally difficult to detect by IHC, unless high concentrations of antibodies were used (data not shown). Using an extended antigen retrieval (37°C overnight following heating in microwave oven), we have obtained clear, albeit somewhat weaker, staining from tissue microarray samples using low concentrations of anti-FOXP3 mAb. However, 13% of normal tissues were not stained, presumably because of harsher fixation conditions. As shown in Figure 1B, a significant reduction was observed among prostate cancer tissues. Furthermore, when the samples with prostate epithelial neoplasia (PIN) were compared with normal tissues, we observed a statistically significant reduction of FOXP3 expression in PIN (Figures S4A and S4B). Taken together, our data demonstrated that FOXP3 downregulation is widespread in prostate cancer and that such downregulation may have occurred at an early stage of prostate cancer.

We then used microdissection to obtain benign prostate tissue and cancer tissues from the same patients and compared the *FOXP3* mRNA levels. Because inflammatory T cells are a major source of FOXP3 expression, we carefully avoided areas of inflammation for dissection. After normalizing against the housekeeping gene, 14 of 18 cases showed 2–10-fold reduction of *FOXP3* mRNA in comparison to the benign tissues (Figure 1C). Six of the 18 samples contain clearly identifiable PIN lesions. We therefore microdissected the PIN lesions and compared the levels of *FOXP3* mRNA transcript with normal and cancerous tissues. As shown in Figure S4C, *FOXP3* transcript is downregulated in PIN lesion. Thus, reduced FOXP3 expression is widespread among prostate cancer samples, perhaps starting at early stage of carcinogenesis.

We used fluorescence in situ hybridization (FISH) to determine *FOXP3* gene deletion in the prostate cancer tissue. As shown in Figure 2 and Table S2, 23 (13.9%) of 165 samples tested showed a deletion of the *FOXP3* gene. Among them, 18 of the 23 cases had a single copy of the X chromosome. However, 5 of the 23 cases showed an increase in the number of X chromosomes. Interestingly, in cells with X polysomy and *FOXP3* deletion, the deletion was complete in all X chromosomes. Thus, X chromosome duplications in cancer tissues likely occurred after deletion of *FOXP3.*

To determine whether *FOXP3* was somatically mutated in primary prostate cancer samples, we isolated cancerous and normal prostate tissues from the same patients and compared the DNA from exons and some exon-intron junctions. A summary of the data is shown in Figure 3A and a representative chromatogram is shown in Figure 3B, with other chromatograms provided in Figure S5. Our sequencing analyses demonstrate single base-pair changes in 5 of 20 samples tested (Table S3). Among them, four were missense mutations, whereas one caused a change in intron 6. One of the missense mutation (K227R) was also reported in the breast cancer (Zuo et al., 2007b). The tumors with the intron 6 mutation showed reduced expression of *FOXP3* (Figure 3C). Among the five samples that contain *FOXP3* mutation in cancer tissue, two contained identifiable PIN lesions. We therefore microdissected the PIN lesion to determine whether the same mutation can be found. As shown in Figure S5, both samples had the same mutations in PIN and cancerous tissues.

To substantiate tumor suppressor activity of *FOXP3*, we transfected *FOXP3* cDNA into prostate cancer cell lines PC3, LNCaP, and Du145. Our data demonstrated strong growth inhibition by FOXP3 (Figures S6 and S7). Importantly, although vector-transfected LNCaP responds to hormone 5α-dihydrotestosterone (5α-DHT), FOXP3 expression abrogated its stimulation by the hormone (Figure S7). The growth inhibition by wild-type (WT) *FOXP3* provided an important functional test for the somatic mutants uncovered from the clinical samples. As shown in Figure 3D, only WT *FOXP3*, but none of the missense mutants, abrogated growth of prostate cancer cell line Du145. Similar data were obtained with another cell line PC3 (data not shown). Therefore, the somatic mutations of the *FOXP3* are functionally inactivated.

FOXP3 is a transcriptional regulator that functions by interacting with DNA in the nuclei (Zuo et al., 2007b). As the first step to understand the mechanism by which the mutations in FOXP3 affect its function, we tagged the FOXP3 protein with the green fluorescence protein (GFP) at the N terminus and visualized its intracellular localization by confocal microscopy. As shown in Figure 3E, three of four somatic mutants disrupted its translocation into nuclei. To substantiate these observations, we isolated cytoplasm, nucleoplasm, and chromatin from PC3 transected with vector control and from WT and somatic *FOXP3* mutant cDNA and determined distribution of FOXP3 by western blot. As shown in Figure 3F, although WT FOXP3 and the V79A mutant reside in both the nucleoplasm and the chromatin, the overwhelming majority of the proteins encoded by other three missense mutants are excluded from the nucleus. Because these three mutations had a more severe impact on the growth

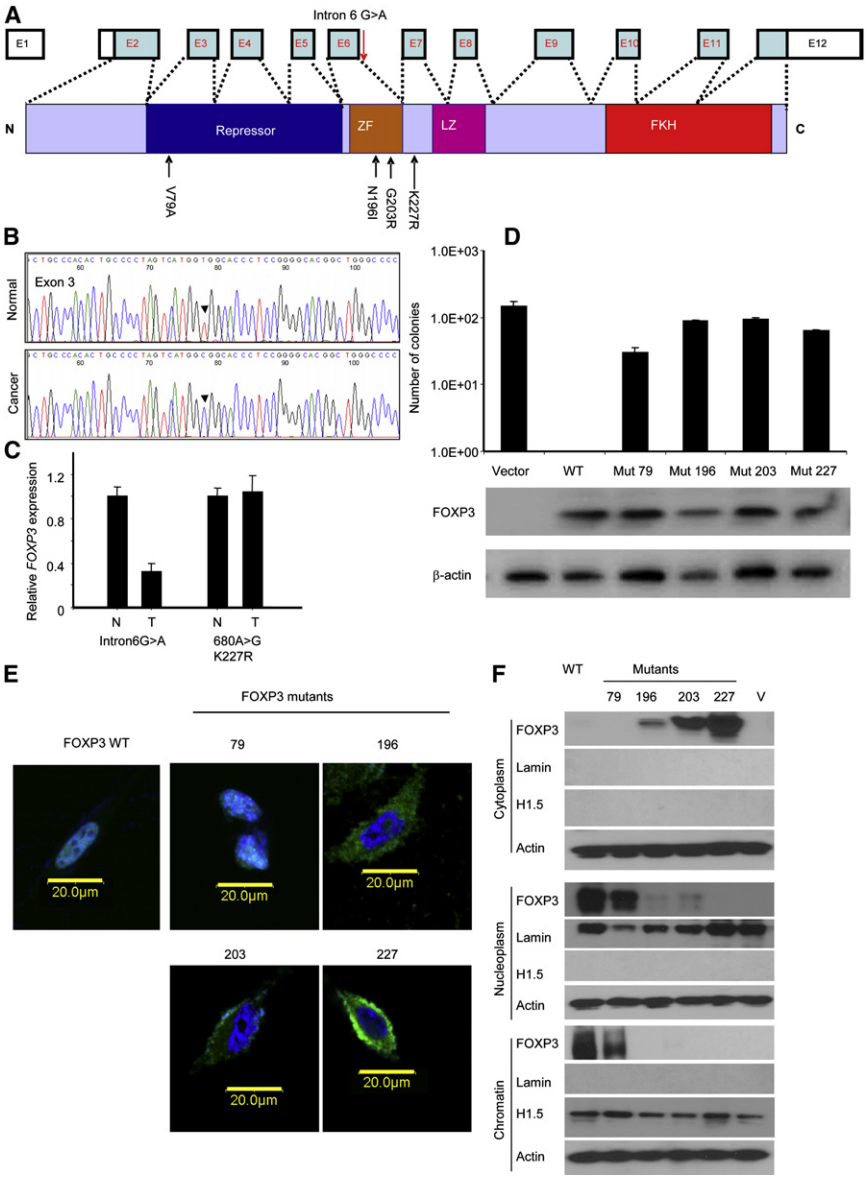

Figure 3. Somatic Mutation of FOXP3 Gene in Prostate Cancer Samples

DNA samples from cancerous and benign tissues dissected from 20 cases of frozen prostate cancer tissues were amplified by PCR and sequenced. The somatic mutants were identified by comparing the DNA sequence of normal and cancerous tissues from the same patients.

(A) Diagram of the *FOXP3* gene showing the position of the somatic mutations identified.

(B) A representative chromatogram showing mutation of *FOXP3* in exon 3.

(C) Partial inactivation of the *FOXP3* locus in prostate cancer with an intronic mutation. Data shown are means and SD of relative levels of *FOXP3* transcripts, with the levels of normal tissues defined as 1.0. This experiment has been repeated once.

(D) Missense mutations of the *FOXP3* gene abrogated inhibition of the colony formation of the prostate cancer cell line Du145 by FOXP3. Data shown are means and SD of colony numbers in 10 cm dishes (n = 3). The expression of FOXP3 is presented underneath the bar graph. This experiment has been repeated at least 3 times.

(E) Impact of missense mutations on nuclear translocation of FOXP3. WT and mutant FOXP3 were tagged with GFP at the N termini and transfected into PC3 cell line. After drug selection to remove untransfected cells, the cells were stained with DAPI to visualize nuclei. Photos shown are merged DAPI and GFP images captured by confocal microscope.

(F) Cellular localization of WT and mutant FOXP3 as measured by western blot after cellular fractionation. The cellular fractions were subject to western blot analysis with anti-FOXP3 mAb (Abcam, ab450) and marker proteins.

inhibition by FOXP3, preventing nuclear localization of FOXP3 appears to be the major mechanism to inactivate the tumor suppressor function. To confirm that disruption of nuclear localization is sufficient to abrogate growth inhibition by FOXP3, we used site-directed mutagenesis to inactivate the known nuclear localization sequence of FOXP3. As shown in Figure S8, mutation in nuclear localization sequence was sufficient to abrogate growth inhibition by FOXP3.

Prostate-Specific Deletion of *FoxP3* Caused Precancerous Lesions

To test the cell-intrinsic effect of *FoxP3* deletion, we crossed the mice with a floxed *FoxP3* locus (diagrammed in Figure 4A) (Fontenot et al., 2005) to a transgenic line that expresses Cre gene under the probasin promoter (PB-Cre4) (Wu et al., 2001). Previous studies have demonstrated that this promoter causes prostate-specific deletion of Floxed genes starting in new-born mice (Wu et al., 2001). Using microdissected tissue samples of 8–12-week-old mice, we observed more than 80% deletion of the *FoxP3* locus among the microdissected prostate epithelial tissue (Figure 4B). The *FoxP3* mRNA was reduced by more than 16 fold (Figure 4C). The less profound reduction in DNA levels likely reflected the fact that our microdissected samples also contained nonepithelial cells that do not express *FoxP3* (Chen et al., 2008). The reduction of FoxP3 protein is confirmed by western blot using the lysates of total prostate (Figure 4D) and immunohistochemistry staining (Figure 4E). Consistent with the kinetics and levels of the *PB-Cre4* transgene expression (Wu et al., 2001), the deletion is more complete in the ventral and lateral prostate lobes than in the anterior and dorsal lobes.

We took several approaches to determine the effect of prostate-specific deletion in the *FoxP3* locus. First, we used magnetic resonance imaging (MRI) to monitor the prostate size in the live mice. As shown in Figure 5A, 12–15-week-old mice with prostate-specific deletion of the *FoxP3* locus had significant enlargement of the prostate. In comparison to WT, a 5-fold increase in the percentage of $Ki67^+$ proliferating epithelial cells was observed in the mutant mice (Figure 5B). Histological

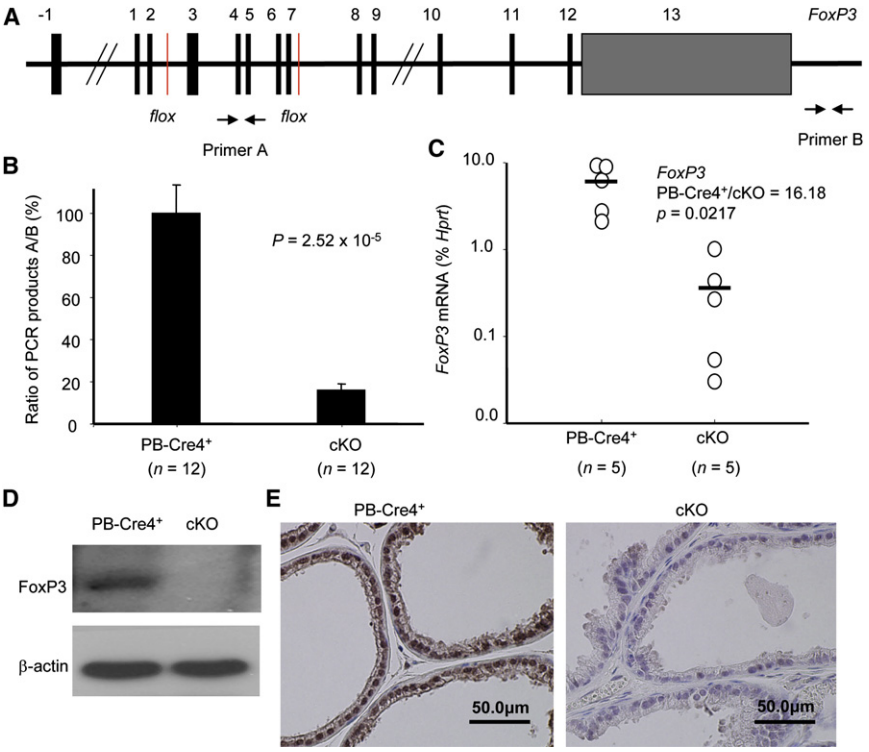

Figure 4. Targeted Deletion of *FoxP3* in the Prostate

(A) Diagram of the floxed *FoxP3* locus and the position of the primers used to measured the ratio of deleted versus undeleted alleles.

(B) Efficient deletion of the *FoxP3* locus in the PB4-Cre4^{+}FoxP3$^{flox/y}$ (cKO) but not the PB-Cre4^{+} FoxP3$^{+/y}$ transgenic mice (p value by an independent-samples t test). Data shown are means and SD of the ratio of product A/product B of DNA isolated from the microdissected prostate epithelium.

(C) Targeted deletion of the *FoxP3* locus caused dramatic reduction of *FoxP3* transcripts in prostate tissue (p value by a Mann-Whitney *U* test). The RNA isolated from microdissected prostate epithelia were quantitated by real-time PCR.

(D) Reduction in FoxP3 expression, as determined by western blot with anti-FoxP3 mAb (hFOXY). Data shown are lysates of prostate tissues from PB-Cre4^{+}FoxP3$^{+/y}$ and PB-Cre4^{+}FoxP3$^{flox/y}$ mice.

(E) Reduction of FoxP3 expression as determined by immunohistochemistry with a polyclonal rabbit anti-mouse FoxP3 antibodies (Poly6238). Staining of ventral prostate lobes is presented. Similar reduction in FoxP3 expression was also observed in lateral prostate. Significant, but less complete, reduction in anterior and dorsal lobes was also found. Data in (B–D) were obtained from tissues of 8–12-week-old mice, whereas those in (E) were obtained from 14–16-week-old mice.

examination of the prostate revealed signs of prostate hyperplasia as early as 14–16 weeks in five of six mutant mice. At 23–26 weeks old, 4 of 5 mutant mice, but none of the six age-matched WT mice, exhibited extensive hyperplasia (Figure 5C and Figure 6A). Early PIN was detectable at 23–26 weeks in a small fraction of ventral and dorsal prostate lobes with *FoxP3* deletion, characterized by increased layers of epithelial cells and nuclear atypia (Figure 5C and data not shown). By 43–60 weeks, all cKO mice examined had hyperplasia. Moreover, all but 1 of 9 cKO mice exhibited early PIN, including multiple layers of epithelial cells (Figures 6B and 6C). The epithelial cells in this region had significantly enlarged nuclei, in comparison to either the single-layered epithelial cells in the same glandular structure (data not shown) or those in the control

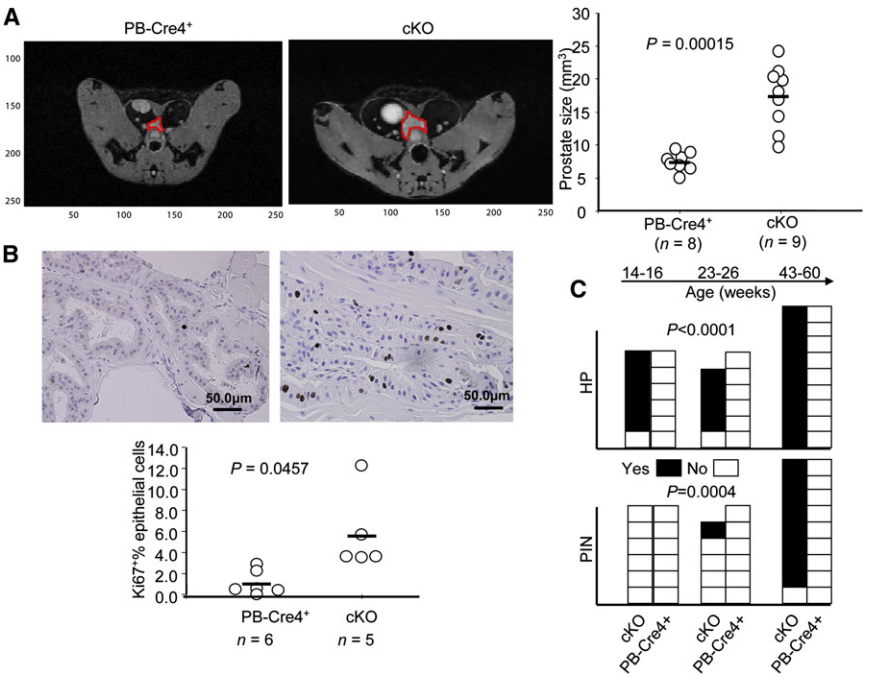

Figure 5. Prostate-Specific Deletion of *FoxP3* in the Prostate Induces Precancerous Lesions

(A) *FoxP3* deletion caused enlargement of prostates. The prostates of 12- to 15-week-old, age-matched WT and condition KO (cKO) mice were measured by magnetic resonance imaging (MRI) (p value by an independent-samples t test). The images of a representative prostate from each group are shown on the left, whereas the prostate volumes of individual mice are shown on the right.

(B) *FoxP3* deletion led to increased proliferation of prostate epithelium, using expression of Ki67 as an indicator of proliferating cells (p value by a Mann-Whitney *U* test). Representative morphology and Ki67 staining are shown at the top, and the percentage of Ki67^{+} cells among the epithelial cells are shown at the bottom. At least five 40× fields for each mouse, at 14–16 weeks of age, were counted.

(C) Incidence of prostate hyperplasia (HP) and prostatic intraepithelial neoplasia (PIN) in cKO (*PB-Cre4^{+}FoxP3$^{flox/y}$*) and in WT (combining both *PB-Cre4^{+}FoxP3$^{+/y}$* and *PB-Cre4^{-}FoxP3$^{flox/y}$*). The statistical significance was determined by a log-rank test.

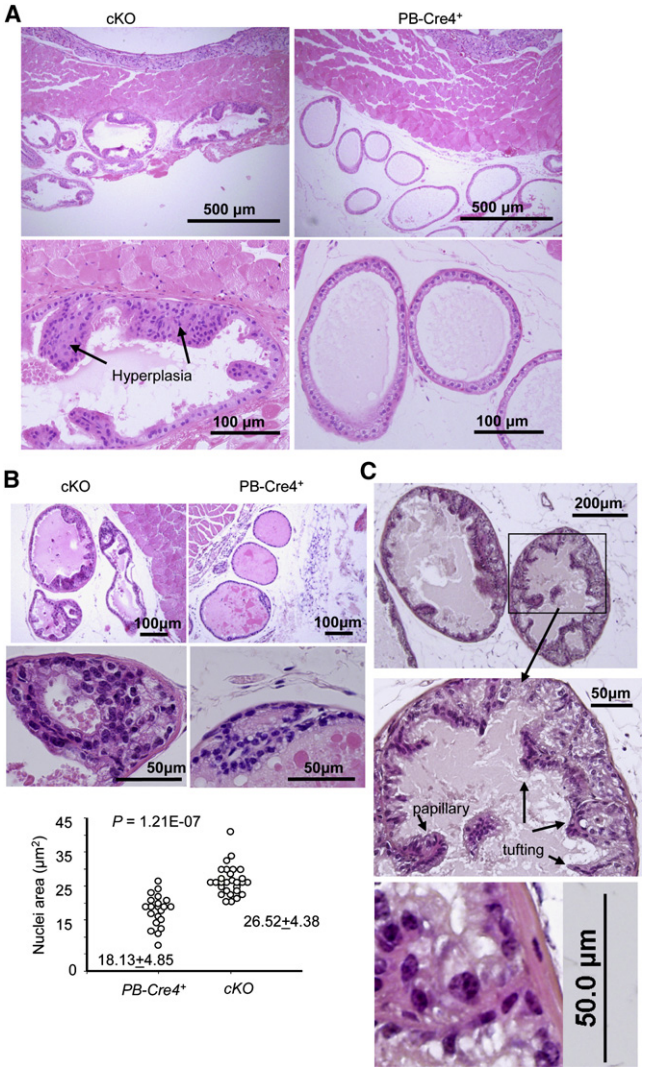

Figure 6. Histology Data of Hyperplasia and Early PIN

(A) Representative H&E staining of hyperplastic lesions in 24-week-old cKO ventral prostate sections. A 26-week-old WT (*PB-Cre4*$^{+}$*FoxP3*$^{+/y}$) ventral prostate image is shown for comparison.

(B) A representative early PIN lesion in ventral prostate of a 43-week-old cKO mouse. The image of an age-matched (*PB-Cre4*$^{+}$*FoxP3*$^{+/y}$) ventral prostate was included for comparison. Low (upper panels) and high (middle panels) power images are presented. The sizes of nuclei were determined by Scion Image software (Scion Corporation, Frederick, Maryland).

(C) A PIN lesion in ventral prostate of a 60-week-old cKO mouse, showing the papillary and tufting. A high-power imagine showing enlarged nuclei and active nucleoli is presented in the lower panel.

mice (Figure 6B, middle and lower panels). In most cases, the epithelia formed both papillary and tufting (Figure 6C) patterns. Under high power, the luminal epithelial cells in these areas appeared transformed, as demonstrated by enlargement of nuclei and more-active nucleoli (Figure 6C). In most mice, multiple PINs were found in the anterior, ventral, and lateral prostate lobes, although the lesions are all focal in nature. All WT prostates have normal morphology through the course of the study. Therefore, targeted mutation of the *FoxP3* gene in prostate tissue is sufficient to initiate the process of prostate cancer development.

FOXP3 Is Necessary and Sufficient to Repress Expression of *MYC*

MYC is overexpressed in 80% of the prostate cancer samples starting as early as benign hyperplasia (Fleming et al., 1986). However, the mechanism by which *MYC* transcription is increased remains unclear. We tested whether *MYC* upregulation correlates with downregulation of the *FOXP3* transcripts. We measured the levels of the mRNA transcripts from microdissected cancerous and benign tissues from 18 patients by real-time PCR. We normalized the transcript levels in cancer tissue against the normal epithelia from the same patients in order to avoid differential RNA degradation under different sample procurement conditions. We observed an increased *MYC* expression in 15 of 18 cases. Importantly, a significant correlation was observed between *FOXP3* downregulation and *MYC* overexpression among malignant tumor samples (Figure 7A). When the levels of normal and cancer tissues were compared separately, a negative correlation between FOXP3 and MYC levels was found in cancer but not normal samples (Figure S9). To test the relevance of this observation in human prostate cells, we tested the effect of the *FOXP3* shRNA on *MYC* expression in early passage primary human prostate epithelial cells. Normal prostate cell culture grew slowly and expressed low levels of MYC. ShRNA silencing increased the growth rate of the culture (Figure S10). As shown in Figure 7B, *FOXP3* shRNA caused a major reduction in the expression of *FOXP3* mRNA and protein. Correspondingly, the levels of *MYC* transcripts and protein were significantly elevated by *FOXP3* shRNA. To test whether the correlation could be causative and independent of cancer development in vivo, we microdissected normal WT and *FoxP3*-deleted prostate tissues and compared the *Myc* transcript levels. As shown in Figure 7C, prostate deletion of the *FOXP3* locus caused a more than 4-fold increase in *Myc* mRNA. Moreover, the increased transcript levels were also reflected in elevation of the Myc protein in the nuclei (Figure 7D). These data demonstrated that FoxP3 is a necessary repressor for the *Myc* locus.

To test whether ectopic expression of FOXP3 is sufficient to repress *MYC*, we transfected two prostate cancer cell lines with FOXP3. As shown in Figure 7E, FOXP3 transfection almost completely abrogated the expression of MYC in both cell lines. To determine whether the growth inhibition was mediated by repression of *MYC*, we cotransfected *FOXP3* with *MYC* cDNA into Du145 cells. The cells were transfected with either pcDNA6-blasticidin vector or *MYC* cDNA (comprising the entire coding region but no untranslated regions) and either the pEF1-G418 vector or *FOXP3* cDNA. As shown in Figure 7F, ectopic expression of *MYC* overcame *FOXP3*-mediated tumor suppression. These data demonstrated that *MYC* repression explains the growth inhibition of FOXP3, at least for established prostate cancer cell line.

Molecular Mechanisms for FOXP3-Mediated *MYC* Repression and for Somatic Inactivation of FOXP3

To understand the mechanism by which FOXP3 represses *MYC*, we used ChIP to identify the site of FOXP3 binding in the *MYC* promoter. As shown in Figure 8A, quantitative PCR analysis indicated that, despite the abundance of forkhead binding sites,

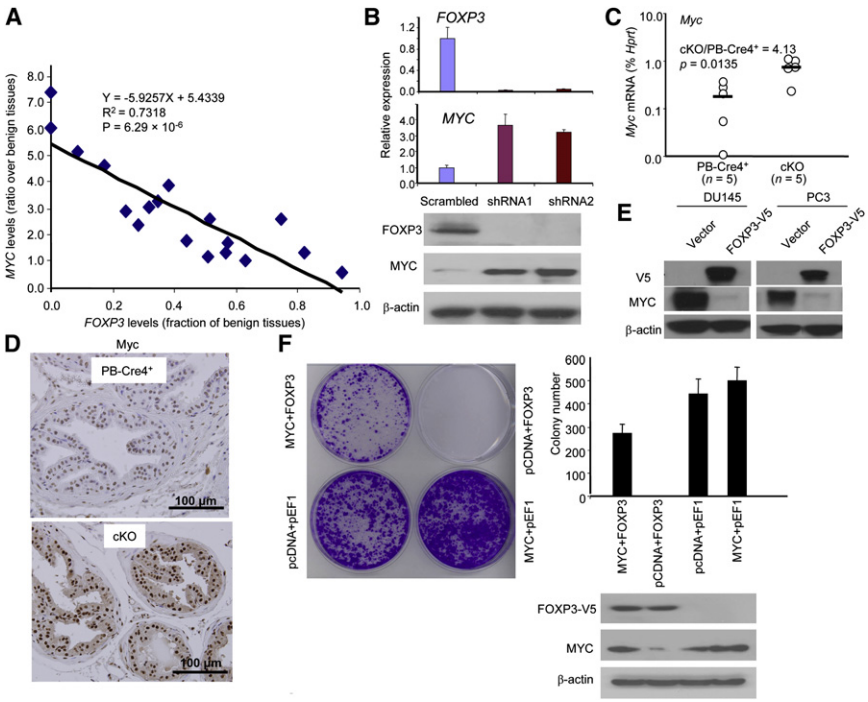

Figure 7. *FOXP3* Is Both Necessary and Sufficient to Repress the *MYC* Oncogene

(A) Inverse correlation between *FOXP3* and *MYC* expression in primary prostate cancer tissues. Statistical significance was observed by using a linear regression model. Data shown are ratio of transcript levels of tumor over benign prostate tissues from the same patients after they were normalized to housekeeping genes. Data from quantitative real-time PCR in 18 cases are presented.

(B) ShRNA silencing of FOXP3 resulted in upregulation of MYC expression in primary HPEC. Early passage HPEC were infected with retroviral vector expressing either control or *FOXP3* shRNA. The uninfected cells were removed by drug selection. At 1 week after infection, the levels of *FOXP3* or *MYC* mRNA were quantitated by real-time PCR. The levels were normalized against *GAPDH*, and those in the control group were defined as 1.0. Data shown are the means and SD of triplicates and were repeated two times. The lower panel shows the levels of FOXP3 and MYC proteins as revealed by western blot.

(C) Targeted deletion of the *FoxP3* locus caused elevation of the *Myc* transcripts in mouse prostate tissue (p value by a Mann-Whitney *U* test). The RNA isolated from microdissected prostate epithelia, from 8- to 12-week-old mice, was quantitated by real-time PCR. Data shown are relative levels of *Myc* mRNA, expressed as a percentage of *Hprt* mRNA.

(D) Immunohistochemistry analysis of Myc expression in PB-Cre4$^+$ and cKO prostate. Data shown are images from dorsal lobes. A comparable elevation was observed in all four lobes.

(E) Ectopic expression of FOXP3 into prostate cancer cell lines repressed MYC expression. PC3 and Du145 cell lines were transfected with V5-tagged FOXP3. After removal of uninfected cells by drug selection, the total cell lysates were analyzed for expression of FOXP3-V5, *MYC*, and β-actin as loading control.

(F) Transfection with *MYC* cDNA prevents FOXP3-mediated growth inhibition. In addition to either control or *FOXP3* cDNA, the tumor cell lines were infected with either control vector or *MYC* plasmid. A representative photograph of cell growth after crystal violet staining is shown on the left; representative data from one of four experiments using the Du145 cell line are presented in the right. Data shown are means and SD of colony numbers in 6 cm dishes (n = 3). The levels of FOXP3 and *MYC* proteins are shown underneath the bar graph. Similar rescue was also found when the PC3 cell line was used (data not shown).

a strong binding of FOXP3 centered around −0.2 kb 5′ of the first transcription-starting site (TSS-P1). To test the significance of this site for the repression, we performed a deletional analysis to map the region that conveys susceptibility to FOXP3 repression. As shown in Figure 8B, little repression by FOXP3 can be observed when the reporter was truncated before the forkead binding site at the −0.2 kb region (F1–F2). Strong inhibition was observed when the binding motif was included (F3–F5). Additional sequences did not increase the efficiency of repression. Sequence alignment revealed a conserved forkhead-binding site surrounding the promoter region with the highest ChIP signal (Figure 8C). When the site was either deleted or mutated, the repression was completely abrogated (Figure 8C). These data demonstrated that FOXP3 represses *MYC* promoter activity by interacting with the forkhead motif at the −0.2 kb 5′ of the *MYC* TSS.

To test whether somatic mutations of *FOXP3* affect *MYC* repression, we transfected WT and mutant *FOXP3* cDNA into the Du145 prostate cancer cell line in conjunction with the *MYC* promoter. Despite similar levels of FOXP3 protein, somatic mutations substantially reduced *MYC* repression (Figure 8D). Because three of the four mutants failed to localize into the nuclei (Figures 8E and 8F), we tested the remaining mutant for its ability to bind to the MYC promoter. As shown in Figure 8E, the V79A mutation significantly reduced the binding of FOXP3 to the *MYC* promoter. Taken together, the data presented in this section demonstrate that FOXP3 represses *MYC* expression by binding the forkhead-binding motif in the promoter. Somatic mutations uncovered in human prostate cancer abrogated the *MYC* repression by either preventing FOXP3's nuclear localization or its binding to a *cis*-element in the *MYC* promoter.

DISCUSSION

Molecular pathogenesis of prostate cancer development includes both upregulation of oncogenes, such as *MYC*, and inactivation of tumor suppressor genes, such as autosomal genes *PTEN* and *NKX3.1*. Although X-linked genes have been implicated by genetic epidemiology and linkage analysis, no X-linked tumor suppressors have been identified for prostate cancer. Our study described herein fills a major gap by identifying the *FOXP3* gene as an X-linked tumor suppressor gene in males.

FOXP3 Is a Tumor Suppressor in Prostate Cancer

We and Rivera et al. have recently reported the involvement of X-linked tumor suppressor genes in female cancer patients, where

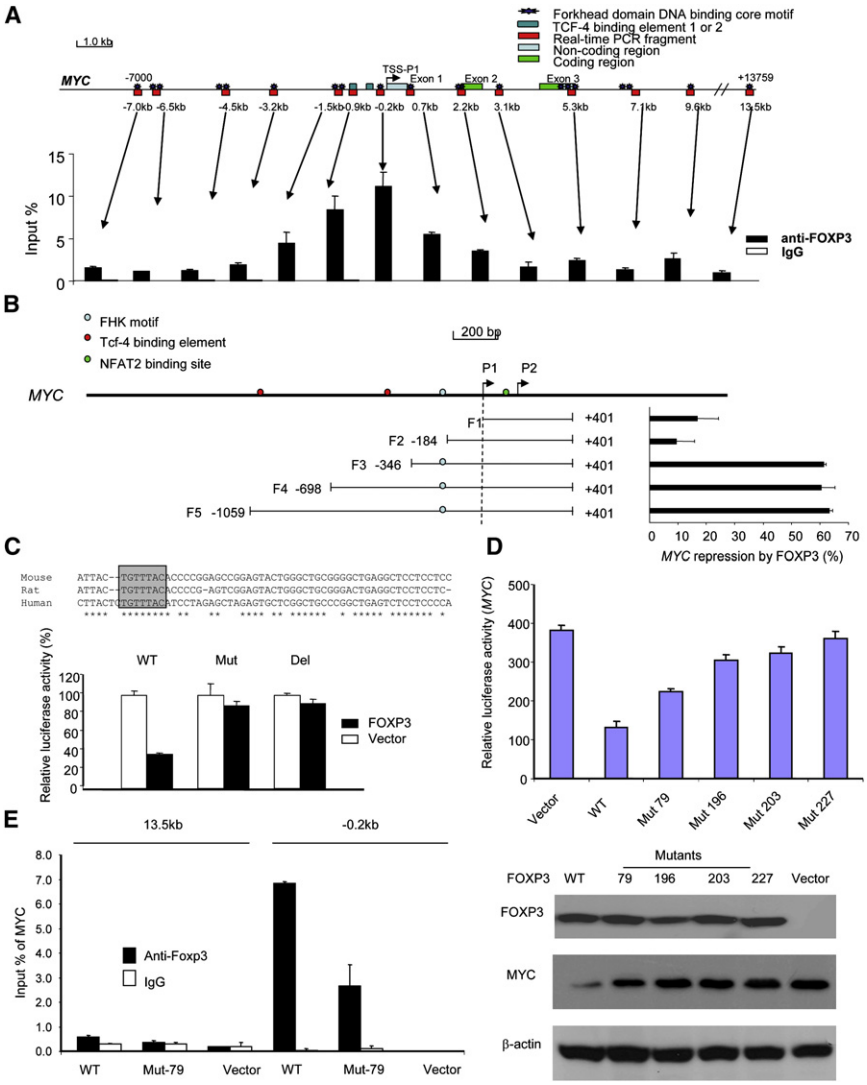

Figure 8. Molecular Mechanism for *MYC* Repression by FOXP3 and Its Inactivation by Mutations in Cancer

(A) Identification of a FOXP3-binding site in the 5′ region of the *MYC* gene. The top panel is a diagram of the *MYC* gene (Bossone et al., 1992), with the Forkhead consensus motifs and the areas covered by PCR primers marked. The distances related to the transcriptional starting site (TSS) are shown. The lower panel shows the amounts of DNA precipitated, expressed as a percentage of input DNA. Data shown were repeated two times.

(B) FOXP3 repressed the *MYC* promoter. The top panel shows a diagram of the *MYC* locus. The lower left panel shows the *MYC* regions included in the luciferase reporter, whereas the lower right panel shows the percentage of inhibition of the promoter activity, expressed as follows: (1 − luciferase activity in the presence of FOXP3/luciferase activity in the absence of FOXP3) × 100. Data shown are means of three independent experiments.

(C) Deletion or mutation of the FOXP3-binding sites abrogated FOXP3-mediated suppression of the *MYC* reporter. The top shows the alignment of human, mouse, and rat *MYC*, revealing that the identified FOXP3-binding motif in *MYC* is in conserved region. The FOXP3-binding motif is shown in the box. The F3 WT reporter or those with either deletion (−195 to −189: TGTTTAC) or mutation (−195 to −189: TGTTTAC to AAAAGGG) of the reporter were transfected into 293T cells in conjunction with either control or FOXP3-expressing vector. The mean luciferase activities in the absence of *FOXP3* cDNA were artificially defined as 100%.

(D) Somatic mutation of FOXP3 reduced its repressor activity for the *MYC* promoter. In the upper panel, the F3 WT reporters were cotransfected with either vector control or cDNA encoding WT or mutant FOXP3 into the 293T cell line. At 48 hr after transfection, the lysates were harvested to measure luciferase activity. Data shown have been reproduced three times. In the lower panel, WT or mutant FOXP3 were transfected into the Du145 cells, and the FOXP3 and MYC protein expression was analyzed by western blot.

(E) Despite normal nuclear translocation, V79A mutant show reduced binding to the critical *cis*-element at −0.2 kb region. Sonicated chromatins isolated from either WT or V79A mutant-transfected Du145 cells were precipitated with either control mouse IgG or mAb specific for FOXP3 (Abcam, ab450). The amounts of specific DNA were quantitated by real-time PCR using primers corresponding to the −0.2 and +13.5 kb regions. Data shown are means percentage input DNA and have been reproduced three times. Error bars in this figure indicate SD.

the suppressor genes are functionally silenced by a programmed epigenetic event that occurred in all cells (X-inactivation) and another lesion such as gene deletion and/or mutation (Rivera et al., 2007; Zuo et al., 2007b). Here, we describe evidence that, in the male, the *FOXP3* locus is silenced by deletion and somatic mutation.

Immunohistochemical analysis demonstrated that the nuclear FOXP3 protein is absent in 68.5% of prostate cancer cases tested. Thus, in addition to deletion and mutation identified herein, additional mechanisms, such as epigenetic silencing or mutations outside the areas analyzed, may also contribute to lack of FOXP3 expression. In contrast, 100% of benign prostate samples exhibited clear epithelial expression of nuclear FOXP3. The overwhelming difference strongly suggests a relationship between FOXP3 downregulation and cancer development. This hypothesis has been confirmed by the impact of prostate-specific deletion of the *FoxP3* locus. These data, together with strong growth inhibition and *MYC* repression by FOXP3, demonstrate that the *FoxP3* gene plays a critical role in suppressing pathological transformation of the prostate. However, it should be pointed out that, similar to other tumor suppressors, including *Trp53* (Chen et al., 2005), *NKX3.1* (Abdulkadir et al., 2002; Kim et al., 2002), and *Pten* (Chen et al., 2005), we have not observed a full spectrum of prostate cancer during 60 weeks of observation. Because FoxP3 regulates *Myc* and because the effect of transgenic *Myc* expression can be either hyperplasia (Zhang

et al., 2000) or carcinoma with gene profiles similar to human prostate cancer (Ellwood-Yen et al., 2003), it is unclear whether extended observation time or additional factors are needed to achieve the full spectrum of prostate cancer. The lack of full carcinogenesis over the observation period makes our model valuable for dissecting the contribution of other factors, such as inflammation and aging, in the pathogenesis of prostate cancer. Nevertheless, the development of prostate hyperplasia and intraepithelial neoplasia, a widely accepted precancerious lesion (Tomlins et al., 2006), demonstrates clearly that inactivation of FOXP3 in prostate cancer patients contributes to prostate cancer development. It is of interest to note that statistically significant downregulation of FOXP3 occurred in the PIN lesion of human samples. Moreover, somatic mutations of FOXP3 were found in both PIN and cancerous lesions. Because deletion of *FoxP3* in the mouse caused early PIN but no cancerous lesions so far, it is likely that *FOXP3* inactivation is an early event in prostate carcinogenesis. Inactivation of *FOXP3* will likely work in concert with additional genetic hits to cause prostate cancer.

FOXP3 exhibits strong growth inhibition of prostate cancer cell lines, which is attenuated by somatic mutations in prostate cancer samples. Therefore, our genetic studies in mice and humans demonstrated a critical role for *FOXP3* as a tumor suppressor gene for prostate cancer. The presence of a X-linked tumor suppressor gene as demonstrated in this study revealed a major exception for the generally accepted two-hit theory of tumor suppressor genes in cancer development (Knudson, 1971).

Because the *FOXP3* resides near a region of a putative prostate cancer susceptibility locus (Gudmundsson et al., 2008), an interesting issue is whether identification of *FOXP3* may help to explain reported X-linked genetic susceptibility to prostate cancer (Monroe et al., 1995). In our analysis of more than 100 probands with familiar prostate cancer, we have so far identified no germline mutation in the coding region of *FOXP3* (data not shown). Given the early onset of lethal autoimmune diseases associated with inactivating mutation of *FOXP3* (Bennett et al., 2001; Chatila et al., 2000; Wildin et al., 2001), it is unlikely that inactivating germline mutation of the FOXP3 gene can be found in prostate cancer patients. Additional analyses are needed to determine whether the *FOXP3* polymorphisms affect susceptibility to prostate cancer.

FOXP3 as a Transcriptional Repressor of Oncogene *MYC*

MYC is arguably the most upregulated oncogene in human cancer, because overexpression has been observed in as many as 30% of all human cancer cases. Our results show frequent overexpression of *MYC* mRNA in prostate cancers, in comparison to adjacent normal epithelia. Although it is clear that a mutation of the *APC* gene resulted in upregulation of *MYC* and although *MYC* is essential for the development of colon cancer associated with *APC* mutation (He et al., 1998; Sansom et al., 2007), *APC* mutation is rare in prostate cancers thus cannot explain a *MYC* overexpression in prostate cancer. Likewise, although MYC overexpression has been observed in all stages of prostate cancer, a low level of gene amplification is observed only in late stages of prostate cancer (Jenkins et al., 1997; Latil et al., 2000). A similar disparity can be observed in other tumor types, including breast and lung cancer (Takahashi et al., 1989; Bieche et al., 1999).

Our data presented here provide strong evidence that FOXP3-mediated repression of *MYC* is necessary to control *MYC* levels in normal prostate epithelial cells and explains much of the widespread overexpression of *MYC* in prostate cancer. Because transgenic expression of *Myc* resulted in the development of prostate cancer with genetic profiles similar to those in human prostate cancer (Ellwood-Yen et al., 2003), disruption of the *MYC* regulator *FOXP3*, as documented here, likely plays a critical role for molecular pathogenesis of human prostate cancer. Nevertheless, using expression array analysis, we have uncovered a large array of genes that are either up- or downregulated by ectopic expression of *FOXP3*. Notably, the genes involved in cancer are the most affected group (Figure S11). Therefore, much like what was observed in breast cancer, FOXP3 will likely suppress development of prostate cancer by targeting multiple genes, including both tumor suppressor and oncogenes (Liu et al., 2009; Zuo et al., 2007a; Zuo et al., 2007b).

EXPERIMENTAL PROCEDURES

Prostate Cancer Samples

Three sources of prostate tissue samples were used for this study. Frozen tissues were obtained from the Prostate Cancer Tissue Bank of Ohio State University with no patient identification information. Tissue microarray samples came from the University of Michigan, Biomax (US Biomax, Inc., Rockville, MD), and Target Biotech (Target Biotech, Inc., Thurmont, MD). All human studies have been approved by the institutional review board of Ohio State University and University of Michigan.

Experimental Animals

Transgenic mice PB-Cre4 expressing the *Cre* cDNA under the control of the probasin promoter have been described elsewhere (Wu et al., 2001) and were obtained from the National Cancer Institute Mouse Model Deposit. Mice with Floxed *FoxP3* locus (Fontenot et al., 2005) were provided by Dr. Alexander Rudensky. Male *PB-Cre4*$^{+/-}$ mice were crossed to female *FoxP3*$^{flox/flox}$ or *FoxP3*$^{flox/+}$ mice. The male F1 mice of given genotypes were used in the study. The pathological evaluation was performed according the Bar Harbor meeting guideline (Shappell et al., 2004). All animal studies have been approved by the University of Michigan Animal User and Carer Committee.

Cell Cultures and Antibodies

Human prostate epithelial cells (HPECs) were purchased from Lonza Group Ltd. (Switzerland) and cultured with medium from the same vendor. Early passage HPECs were infected with retrovirus expressing either control shRNA or *FOXP3* shRNA vector. Two FOXP3 short hairpin RNA (shRNA) constructs are FOXP3-993-shRNA and FOXP3-1355-shRNA (GenBank accession number NM_014009). Oligonucleotides encoding small interfering RNA (siRNA) directed against FOXP3 are 5′-GCTTCATCTGTGGCATCATCC-3′ for FOXP3-993-shRNA (993–1013 nucleotides from TSS) and 5′-GAGTCTGC ACAAGTGCTTTGT-3′ for FOXP3-1355-shRNA (1355–1375 from TSS). The selected shRNA oligonucleotides were cloned into pSIREN-RetroQ vectors (Clontech, Mountain View, CA) to generate siRNA according to manufacturer's protocol. Prostate cancer cell lines Du145 and PC3 were obtained from the American Type Culture Collection (ATCC, Rockville, MD). Antibodies specific for the following targets were used for the study: cMyc (Santa Cruz Biotechnology, Santa Cruz, CA; catalog number sc-40), FOXP3 (Abcam, ab20034 for IHC and ab450 for western blot, Cambridge, MA), hFOXY (eBioscience, catalog number 14-5779-82 for western blot in HPEC), anti-V5 (Invitrogen, SKU number R960-25), Ki67 (Dako Cytomation, code number M7249, Carpenteria, CA), β-actin (Sigma, catalog number A5441, St. Louis, MO), and anti-IgG (Santa Cruz Biotechnology, Santa Cruz, CA).

Immunohistochemistry

Because *FOXP3* is expressed at lower levels in epithelial cells than in the regulatory T cells, the conditions typically used for detecting Treg cells in tumor samples do not give reproducible staining in the epithelial cells. To facilitate replication of the current studies, we have screened commercially available anti-FOXP3 antibodies and established staining conditions that give strong staining of FOXP3 in human and mouse epithelial cells.

The normal and cancer prostate frozen samples were partially thawed at room temperature and then immersed in 10% formalin for 8–12 hr and embedded in paraffin. Antigens were retrieved by microwave in 1× target retrieval buffer (Dako) for 12 min. For TMA samples, antigens were retrieved at 37°C overnight after the microwave antigen retrieval treatment. ABC detection system was used for immunostaining according to the manufacturer's protocol (Vectastain Elite ABC, Burlingame, CA). The incubation time for primary antibody FOXP3 (Abcam 236A/E7, 1:100), FoxP3 (BioLegend Poly6238, 1:100), c-Myc (Santa Cruz Biotechnology 9E10, 1:200), c-Myc (Abcam ab39688, 1:100), and Ki67 (Dako TEC-3, 1:100) was overnight at 4°C. After incubation with primary antibody, staining was followed by ABC detection system using biotinylated anti-mouse/rabbit/rat IgG. AEC was used as chromogen. The slides were counterstained with hematoxylin and mounted in xylene mounting medium for examination.

Statistical Analysis

The distribution of samples for each group was evaluated using a one-sample Kolmogorov-Smirnov test. In the samples with normal distributions, we compared the means of the dependent variable using a paired-samples t test and means of the independent variable using an independent-samples t test between two groups. In the samples with nonnormal distribution, we compared the means of the independent variable between two groups using a Mann-Whitney *U* test. Chi-square test was used to compare the relationship between the expression of FOXP3 and MYC among patients. The relationship between the levels of gene expression was estimated using a linear regression model. All data were entered into an access database and analyzed using the Excel 2000 and SPSS (version 10.0; SPSS, Inc.) software.

ACCESSION NUMBERS

The raw data for Figure S11 have been submitted to ArrayExpress under accession number E-MTAB-108.

SUPPLEMENTAL DATA

Supplemental data include four tables, 11 figures, and Supplemental Experimental Procedures and can be found with this article online at http://www.cell.com/cancer-cell/supplemental/S1535-6108(09)00263-3.

ACKNOWLEDGMENTS

We thank Dr. Alexander Rudensky for the *FoxP3*$^{flox/flox}$ mice, Dr. Hong Wu, Jianti Huang from UCLA, and Dr. George V. Thomas from Institute of Cancer Research and Royal Marsden Hospital, UK, for pathological evaluation of mouse prostate; Drs. Eric Fearon, Steve Gruber, Michael Sabel, and Yuan Zhu for valuable discussion and critical reading of the manuscript; and Ms Darla Kroft for editorial assistance. This study is supported by grants from NIH, Department of Defense, Cancer Research Institute in New York, American Cancer Society, and by a gift made the University of Michigan Cancer Center.

Received: December 12, 2008
Revised: May 8, 2009
Accepted: August 17, 2009
Published: October 5, 2009

REFERENCES

Abdulkadir, S.A., Magee, J.A., Peters, T.J., Kaleem, Z., Naughton, C.K., Humphrey, P.A., and Milbrandt, J. (2002). Conditional loss of Nkx3.1 in adult mice induces prostatic intraepithelial neoplasia. Mol. Cell. Biol. *22*, 1495–1503.

Amundadottir, L.T., Sulem, P., Gudmundsson, J., Helgason, A., Baker, A., Agnarsson, B.A., Sigurdsson, A., Benediktsdottir, K.R., Cazier, J.B., Sainz, J., et al. (2006). A common variant associated with prostate cancer in European and African populations. Nat. Genet. *38*, 652–658.

Bar-Shira, A., Matarasso, N., Rosner, S., Bercovich, D., Matzkin, H., and Orr-Urtreger, A. (2006). Mutation screening and association study of the candidate prostate cancer susceptibility genes MSR1, PTEN, and KLF6. Prostate *66*, 1052–1060.

Bennett, C.L., Christie, J., Ramsdell, F., Brunkow, M.E., Ferguson, P.J., Whitesell, L., Kelly, T.E., Saulsbury, F.T., Chance, P.F., and Ochs, H.D. (2001). The immune dysregulation, polyendocrinopathy, enteropathy, X-linked syndrome (IPEX) is caused by mutations of FOXP3. Nat. Genet. *27*, 20–21.

Bieche, I., Laurendeau, I., Tozlu, S., Olivi, M., Vidaud, D., Lidereau, R., and Vidaud, M. (1999). Quantitation of MYC gene expression in sporadic breast tumors with a real-time reverse transcription-PCR assay. Cancer Res. *59*, 2759–2765.

Bommer, G.T., and Fearon, E.R. (2007). Role of c-Myc in Apc mutant intestinal phenotype: case closed or time for a new beginning? Cancer Cell *11*, 391–394.

Bossone, S.A., Asselin, C., Patel, A.J., and Marcu, K.B. (1992). MAZ, a zinc finger protein, binds to c-MYC and C2 gene sequences regulating transcriptional initiation and termination. Proc. Natl. Acad. Sci. USA *89*, 7452–7456.

Chatila, T.A., Blaeser, F., Ho, N., Lederman, H.M., Voulgaropoulos, C., Helms, C., and Bowcock, A.M. (2000). JM2, encoding a fork head-related protein, is mutated in X-linked autoimmunity-allergic disregulation syndrome. J. Clin. Invest. *106*, R75–R81.

Chen, G.Y., Chen, C., Wang, L., Chang, X., Zheng, P., and Liu, Y. (2008). Cutting edge: broad expression of the FoxP3 locus in epithelial cells: a caution against early interpretation of fatal inflammatory diseases following in vivo depletion of FoxP3-expressing cells. J. Immunol. *180*, 5163–5166.

Chen, Z., Trotman, L.C., Shaffer, D., Lin, H.K., Dotan, Z.A., Niki, M., Koutcher, J.A., Scher, H.I., Ludwig, T., Gerald, W., et al. (2005). Crucial role of p53-dependent cellular senescence in suppression of Pten-deficient tumorigenesis. Nature *436*, 725–730.

Dalla-Favera, R., Bregni, M., Erikson, J., Patterson, D., Gallo, R.C., and Croce, C.M. (1982). Human c-myc onc gene is located on the region of chromosome 8 that is translocated in Burkitt lymphoma cells. Proc. Natl. Acad. Sci. USA *79*, 7824–7827.

Ellwood-Yen, K., Graeber, T.G., Wongvipat, J., Iruela-Arispe, M.L., Zhang, J., Matusik, R., Thomas, G.V., and Sawyers, C.L. (2003). Myc-driven murine prostate cancer shares molecular features with human prostate tumors. Cancer Cell *4*, 223–238.

Emmert-Buck, M.R., Vocke, C.D., Pozzatti, R.O., Duray, P.H., Jennings, S.B., Florence, C.D., Zhuang, Z., Bostwick, D.G., Liotta, L.A., and Linehan, W.M. (1995). Allelic loss on chromosome 8p12-21 in microdissected prostatic intraepithelial neoplasia. Cancer Res. *55*, 2959–2962.

Erikson, J., ar-Rushdi, A., Drwinga, H.L., Nowell, P.C., and Croce, C.M. (1983). Transcriptional activation of the translocated c-myc oncogene in burkitt lymphoma. Proc. Natl. Acad. Sci. USA *80*, 820–824.

Fearon, E.R., and Dang, C.V. (1999). Cancer genetics: tumor suppressor meets oncogene. Curr. Biol. *9*, R62–R65.

Fleming, W.H., Hamel, A., MacDonald, R., Ramsey, E., Pettigrew, N.M., Johnston, B., Dodd, J.G., and Matusik, R.J. (1986). Expression of the c-myc protooncogene in human prostatic carcinoma and benign prostatic hyperplasia. Cancer Res. *46*, 1535–1538.

Fontenot, J.D., Gavin, M.A., and Rudensky, A.Y. (2003). Foxp3 programs the development and function of CD4+CD25+ regulatory T cells. Nat. Immunol. *4*, 330–336.

Fontenot, J.D., Rasmussen, J.P., Williams, L.M., Dooley, J.L., Farr, A.G., and Rudensky, A.Y. (2005). Regulatory T cell lineage specification by the forkhead transcription factor foxp3. Immunity *22*, 329–341.

Fox, S.B., Launchbury, R., Bates, G.J., Han, C., Shaida, N., Malone, P.R., Harris, A.L., and Banham, A.H. (2007). The number of regulatory T cells in prostate cancer is associated with the androgen receptor and hypoxia-inducible factor (HIF)-2alpha but not HIF-1alpha. Prostate *67*, 623–629.

Grandori, C., Cowley, S.M., James, L.P., and Eisenman, R.N. (2000). The Myc/Max/Mad network and the transcriptional control of cell behavior. Annu. Rev. Cell Dev. Biol. *16*, 653–699.

Gudmundsson, J., Sulem, P., Manolescu, A., Amundadottir, L.T., Gudbjartsson, D., Helgason, A., Rafnar, T., Bergthorsson, J.T., Agnarsson, B.A., Baker, A., et al. (2007). Genome-wide association study identifies a second prostate cancer susceptibility variant at 8q24. Nat. Genet. *39*, 631–637.

Gudmundsson, J., Sulem, P., Rafnar, T., Bergthorsson, J.T., Manolescu, A., Gudbjartsson, D., Agnarsson, B.A., Sigurdsson, A., Benediktsdottir, K.R., Blondal, T., et al. (2008). Common sequence variants on 2p15 and Xp11.22 confer susceptibility to prostate cancer. Nat. Genet. *40*, 281–283.

Haiman, C.A., Le Marchand, L., Yamamato, J., Stram, D.O., Sheng, X., Kolonel, L.N., Wu, A.H., Reich, D., and Henderson, B.E. (2007a). A common genetic risk factor for colorectal and prostate cancer. Nat. Genet. *39*, 954–956.

Haiman, C.A., Patterson, N., Freedman, M.L., Myers, S.R., Pike, M.C., Waliszewska, A., Neubauer, J., Tandon, A., Schirmer, C., McDonald, G.J., et al. (2007b). Multiple regions within 8q24 independently affect risk for prostate cancer. Nat. Genet. *39*, 638–644.

He, T.C., Sparks, A.B., Rago, C., Hermeking, H., Zawel, L., da Costa, L.T., Morin, P.J., Vogelstein, B., and Kinzler, K.W. (1998). Identification of c-MYC as a target of the APC pathway. Science *281*, 1509–1512.

Hori, S., Nomura, T., and Sakaguchi, S. (2003). Control of regulatory T cell development by the transcription factor Foxp3. Science *299*, 1057–1061.

Jenkins, R.B., Qian, J., Lieber, M.M., and Bostwick, D.G. (1997). Detection of c-myc oncogene amplification and chromosomal anomalies in metastatic prostatic carcinoma by fluorescence in situ hybridization. Cancer Res. *57*, 524–531.

Kim, M.J., Cardiff, R.D., Desai, N., Banach-Petrosky, W.A., Parsons, R., Shen, M.M., and Abate-Shen, C. (2002). Cooperativity of Nkx3.1 and Pten loss of function in a mouse model of prostate carcinogenesis. Proc. Natl. Acad. Sci. USA *99*, 2884–2889.

Knudson, A.G., Jr. (1971). Mutation and cancer: statistical study of retinoblastoma. Proc. Natl. Acad. Sci. USA *68*, 820–823.

Kolligs, F.T., Hu, G., Dang, C.V., and Fearon, E.R. (1999). Neoplastic transformation of RK3E by mutant beta-catenin requires deregulation of Tcf/Lef transcription but not activation of c-myc expression. Mol. Cell. Biol. *19*, 5696–5706.

Latil, A., Vidaud, D., Valeri, A., Fournier, G., Vidaud, M., Lidereau, R., Cussenot, O., and Biache, I. (2000). htert expression correlates with MYC over-expression in human prostate cancer. Int. J. Cancer *89*, 172–176.

Liu, R., Wang, L., Chen, G., Katoh, H., Chen, C., Liu, Y., and Zheng, P. (2009). FOXP3 up-regulates p21 expression by site-specific inhibition of histone deacetylase 2/histone deacetylase 4 association to the locus. Cancer Res. *69*, 2252–2259.

Lu, X., Park, S.H., Thompson, T.C., and Lane, D.P. (1992). Ras-induced hyperplasia occurs with mutation of p53, but activated ras and myc together can induce carcinoma without p53 mutation. Cell *70*, 153–161.

Monroe, K.R., Yu, M.C., Kolonel, L.N., Coetzee, G.A., Wilkens, L.R., Ross, R.K., and Henderson, B.E. (1995). Evidence of an X-linked or recessive genetic component to prostate cancer risk. Nat. Med. *1*, 827–829.

Narla, G., Difeo, A., Reeves, H.L., Schaid, D.J., Hirshfeld, J., Hod, E., Katz, A., Isaacs, W.B., Hebbring, S., Komiya, A., et al. (2005). A germline DNA polymorphism enhances alternative splicing of the KLF6 tumor suppressor gene and is associated with increased prostate cancer risk. Cancer Res. *65*, 1213–1222.

Narla, G., Heath, K.E., Reeves, H.L., Li, D., Giono, L.E., Kimmelman, A.C., Glucksman, M.J., Narla, J., Eng, F.J., Chan, A.M., et al. (2001). KLF6, a candidate tumor suppressor gene mutated in prostate cancer. Science *294*, 2563–2566.

Rivera, M.N., Kim, W.J., Wells, J., Driscoll, D.R., Brannigan, B.W., Han, M., Kim, J.C., Feinberg, A.P., Gerald, W.L., Vargas, S.O., et al. (2007). An X chromosome gene, WTX, is commonly inactivated in Wilms tumor. Science *315*, 642–645.

Roncador, G., Brown, P.J., Maestre, L., Hue, S., Martinez-Torrecuadrada, J.L., Ling, K.L., Pratap, S., Toms, C., Fox, B.C., Cerundolo, V., et al. (2005). Analysis of FOXP3 protein expression in human CD4+CD25+ regulatory T cells at the single-cell level. Eur. J. Immunol. *35*, 1681–1691.

Sansal, I., and Sellers, W.R. (2004). The biology and clinical relevance of the PTEN tumor suppressor pathway. J. Clin. Oncol. *22*, 2954–2963.

Sansom, O.J., Meniel, V.S., Muncan, V., Phesse, T.J., Wilkins, J.A., Reed, K.R., Vass, J.K., Athineos, D., Clevers, H., and Clarke, A.R. (2007). Myc deletion rescues Apc deficiency in the small intestine. Nature *446*, 676–679.

Shappell, S.B., Thomas, G.V., Roberts, R.L., Herbert, R., Ittmann, M.M., Rubin, M.A., Humphrey, P.A., Sundberg, J.P., Rozengurt, N., Barrios, R., et al. (2004). Prostate pathology of genetically engineered mice: definitions and classification. The consensus report from the Bar Harbor meeting of the Mouse Models of Human Cancer Consortium Prostate Pathology Committee. Cancer Res. *64*, 2270–2305.

Spatz, A., Borg, C., and Feunteun, J. (2004). X-chromosome genetics and human cancer. Nat. Rev. Cancer *4*, 617–629.

Suzuki, H., Freije, D., Nusskern, D.R., Okami, K., Cairns, P., Sidransky, D., Isaacs, W.B., and Bova, G.S. (1998). Interfocal heterogeneity of PTEN/MMAC1 gene alterations in multiple metastatic prostate cancer tissues. Cancer Res. *58*, 204–209.

Takahashi, T., Obata, Y., Sekido, Y., Hida, T., Ueda, R., Watanabe, H., Ariyoshi, Y., Sugiura, T., and Takahashi, T. (1989). Expression and amplification of myc gene family in small cell lung cancer and its relation to biological characteristics. Cancer Res. *49*, 2683–2688.

Taub, R., Kirsch, I., Morton, C., Lenoir, G., Swan, D., Tronick, S., Aaronson, S., and Leder, P. (1982). Translocation of the c-myc gene into the immunoglobulin heavy chain locus in human Burkitt lymphoma and murine plasmacytoma cells. Proc. Natl. Acad. Sci. USA *79*, 7837–7841.

Thompson, T.C., Southgate, J., Kitchener, G., and Land, H. (1989). Multistage carcinogenesis induced by ras and myc oncogenes in a reconstituted organ. Cell *56*, 917–930.

Tomlins, S.A., Rubin, M.A., and Chinnaiyan, A.M. (2006). Integrative biology of prostate cancer progression. Annu. Rev. Pathol. *1*, 243–271.

Vocke, C.D., Pozzatti, R.O., Bostwick, D.G., Florence, C.D., Jennings, S.B., Strup, S.E., Duray, P.H., Liotta, L.A., Emmert-Buck, M.R., and Linehan, W.M. (1996). Analysis of 99 microdissected prostate carcinomas reveals a high frequency of allelic loss on chromosome 8p12-21. Cancer Res. *56*, 2411–2416.

Wildin, R.S., Ramsdell, F., Peake, J., Faravelli, F., Casanova, J.L., Buist, N., Levy-Lahad, E., Mazzella, M., Goulet, O., Perroni, L., et al. (2001). X-linked neonatal diabetes mellitus, enteropathy and endocrinopathy syndrome is the human equivalent of mouse scurfy. Nat. Genet. *27*, 18–20.

Witte, J.S. (2007). Multiple prostate cancer risk variants on 8q24. Nat. Genet. *39*, 579–580.

Wong, A.J., Ruppert, J.M., Eggleston, J., Hamilton, S.R., Baylin, S.B., and Vogelstein, B. (1986). Gene amplification of c-myc and N-myc in small cell carcinoma of the lung. Science *233*, 461–464.

Wu, X., Wu, J., Huang, J., Powell, W.C., Zhang, J., Matusik, R.J., Sangiorgi, F.O., Maxson, R.E., Sucov, H.M., and Roy-Burman, P. (2001). Generation of a prostate epithelial cell-specific Cre transgenic mouse model for tissue-specific gene ablation. Mech. Dev. *101*, 61–69.

Xu, J., Meyers, D., Freije, D., Isaacs, S., Wiley, K., Nusskern, D., Ewing, C., Wilkens, E., Bujnovszky, P., Bova, G.S., et al. (1998). Evidence for a prostate cancer susceptibility locus on the X chromosome. Nat. Genet. *20*, 175–179.

Yeager, M., Orr, N., Hayes, R.B., Jacobs, K.B., Kraft, P., Wacholder, S., Minichiello, M.J., Fearnhead, P., Yu, K., Chatterjee, N., et al. (2007). Genome-wide association study of prostate cancer identifies a second risk locus at 8q24. Nat. Genet. *39*, 645–649.

Zhang, X., Lee, C., Ng, P.Y., Rubin, M., Shabsigh, A., and Buttyan, R. (2000). Prostatic neoplasia in transgenic mice with prostate-directed overexpression of the c-myc oncoprotein. Prostate *43*, 278–285.

Zuo, T., Liu, R., Zhang, H., Chang, X., Liu, Y., Wang, L., Zheng, P., and Liu, Y. (2007a). FOXP3 is a novel transcription repressor for the breast cancer oncogene SKP2. J. Clin. Invest. *117*, 3765–3773.

Zuo, T., Wang, L., Morrison, C., Chang, X., Zhang, H., Li, W., Liu, Y., Wang, Y., Liu, X., Chan, M.W.Y., et al. (2007b). FOXP3 is an X-linked breast cancer suppressor gene and an important repressor of HER-2/ErbB2 oncogene. Cell *129*, 1275–1286.